

WITHDRAWN: Double layer polarization insensitive rGO absorber for side lobe suppression of two-dimensional antenna array

Surekha Rani

surekhagarg9@gmail.com

Chandigarh University

Anupma Marwaha

Sant Longowal Institute of Engg. and Technology

Sanjay Marwaha

Sant Longowal Institute of Engg. and Technology

Research Article

Keywords: reduced graphene oxides, electromagnetic absorber, antenna array, side lobes, effective bandwidth, directivity

Posted Date: April 20th, 2022

DOI: <https://doi.org/10.21203/rs.3.rs-1535787/v1>

License:   This work is licensed under a Creative Commons Attribution 4.0 International License. [Read Full License](#)

Additional Declarations: No competing interests reported.

EDITORIAL NOTE:

The full text of this preprint has been withdrawn by the authors while they make corrections to the work. Therefore, the authors do not wish this work to be cited as a reference. Questions should be directed to the corresponding author.

Abstract

Reduced graphene oxides based double layer polarization insensitive electromagnetic absorber has been integrated with two-dimensional antenna array to reduce the interference from side lobes and to decrease the bit error rate of array signal which ultimately leads to enhanced antenna array performance. 2×8 elements antenna array has been designed on aluminium oxide substrate having dielectric constant $\epsilon_r = 9.8$ used for advanced radio function conceptual based multi-function X-band radar applications. Reduced graphene oxides based microwave absorber consists of matched layer and lossy layer having 16 GHz effective wide bandwidth from 2 GHz to 18 GHz at normal incident angle for transverse electric mode. The frequency compatible absorber when integrated with antenna array on same substrate leads to reduction in number of side lobes as well as side lobe levels of array and from results, it has been authenticated that antenna array gain and directivity has been greatly improved.

1. Introduction

The exponential growth in wireless fidelity systems and modern automation equipment facilitates the standard of living but accompanying electromagnetic pollution deteriorate the quality of life by spreading chronic diseases [1–3]. Declined performance of electronic gadgets due to electromagnetic interference effects demands for high-performance microwave absorber having wider absorption bandwidth, polarization insensitive with low surface to volume density and high melting temperature [4–7]. The conventional single layer absorbers are sometimes not adequate to meet the industrial and commercial requirements, thus multilayer absorber using state of art low dimensional materials (1-D and 2-D) and nanocomposites are becoming popular recently [8–10].

Renchao Hu et al. fabricated the cobalt blended amorphous microwires and $\text{Ce}_2\text{Fe}_{17}\text{N}_3$ composites based electromagnetic absorber for X band having 3.6 GHz absorption bandwidth. Authors explained that the synergistic effect between cobalt nanowires and $\text{Ce}_2\text{Fe}_{17}\text{N}_3$ /silicone composite reduced the reflection coefficient of electromagnetic absorber and enhanced the absorption characteristics which results in better absorption performance [11]. Further some authors also focus on geometry based absorbers for enhancing the absorption properties. Ruixiang Deng et al. proposed the lossy wheel like metasurface which has 90% absorption for the frequency at 6 GHz to 16.5 GHz. Authors revealed that the absorption properties of reported absorber enhanced due to the additive effects of ohmic loss caused by lossy wheel type metasurface and dielectric loss due to PVC (polyvinyl Chloride) substrate. Further authors explained that ohmic loss dominates the dielectric loss and conductive areas of metasurface parallel to external electric field mainly dissipate energy and symmetric structure of lossy wheels makes the absorber polarization insensitive [12]. Guangzhen Cui et al. fabricated the lightweight hollow reduced graphite oxide (rGO) blended in Fe_3O_4 nanocomposites using solvothermal technology. The physical crystal structure and dimensions of reported nanocomposites are characterized with X ray diffraction method and scanning electronic microscopy method. Further authors claimed that proposed hollow nanocomposites when blended with graphene becomes extremely light weight and wide band as compared to Fe_3O_4 nanocomposites alone. Reflection coefficient dip of value -41.89 dB at 6.7 GHz has been reported alongwith 10.2 GHz effective absorption bandwidth from 3.4 GHz to 13.6 GHz. However, authors have not explored the polarization insensitive properties of their absorber [13].

In proposed work, double layer electromagnetic absorber structure has been designed which is based on epoxy resin material blended with reduced graphene oxide nanomaterial particles. Reduced graphene oxide (rGO) is synthesised from graphene using modified Hummers' method. In this method [25] graphite flakes were treated with concentrated Sulfuric acid (98%) and Phosphoric acid contents to obtain rGO. So, rGO is derived from graphene hence it has inherent absorption properties of graphene. Graphene has unique atomic structure, favours working it as a microwave absorber because three out of the four valence electrons in graphene contribute toward σ bond with neighbour atoms, viewed as

2-D tightly packed honeycomb lattice [26, 27]. The honeycomb geometry is desirable for electromagnetic wave dissipation via absorption. In addition to that, fourth delocalized, perpendicularly oriented valence electron participates in π bond, resulting in high surface resistance of graphene as compared to metals, which mainly contributes to absorption of EM wave in terms of heat [28]. However, the microwave attenuation by pure graphene is difficult due to poor impedance matching from the single dielectric loss. Excellent microwave absorption generally requires efficient synergism between the relative permittivity and permeability [29]. Therefore, in proposed work dual layer rGO absorber is proposed, in which matching layer is dedicated for good impedance matching. Further, as per the article written by Jesus de La Fuente (CEO Graphenea), in large scale of operation where scientists need to utilize huge quantity of graphene mainly for industrial applications like energy conservation or dissipation, reduced graphene oxide is mostly used because of its cost effectiveness, but rGO has poor yields in terms of surface area and electronic conductivity. Therefore, to optimize both parameters i.e. cost and performance of reduced graphene oxide absorber, the proposed absorber structure consists of matched layer followed by absorbing or lossy layers backed by perfect electric conductor sheet. Both layers are made from reduced graphene oxide particles but with different particle size and weight percentage. To check whether the designed absorber is polarization sensitive or not, various plots of reflection coefficients are plotted at different incident angles in transverse electric (TE) and transverse magnetic (TM) modes. To validate the applicability of absorber, an antenna array operating in X band has been designed for radar applications. The wave model of dual layer absorber has been demonstrated analytically and further simulation model of the proposed absorber integrated between array elements of antenna array structure has been developed with the help of high-frequency structure simulator (HFSS). The performance is then analyzed by evaluating absorber reflection coefficient, gain and directivity of the antenna array with and without absorber. The comparison results show that array performance has been greatly enhanced on application of absorber due to reduction of interelement waves travelling from one array element to another.

2. Modelling Of Double Layer Absorber Structure

The sequence of two layers have been placed above the perfect electric conductor (PEC) sheet for designing of electromagnetic wave absorber. The value of reflection coefficient at first layer is of great importance. The lesser the value of reflection coefficient at air-absorber interface, better will be the absorption performance [14]. The amplitudes of incident, reflected and transmitted powers through absorber structures have been calculated and various reflection coefficient graphs have been plotted at both normal and oblique incident angles to verify absorber performance.

The electromagnetic wave model of proposed double-layer absorber structure has been discussed for transverse electric (TE) mode here. In the model, the air-absorber interfacing layer and matched-lossy layer are assumed to be extremely thin resistive sheets of negligible thickness of conductance G_1 and G_2 respectively as shown in Fig. 1. The general equation of electric field intensity \vec{E} and magnetic field intensity \vec{H} for any arbitrary layer, x , having admittance Y can be expressed as follows [15]:

$$\vec{E} = P_i e^{-jk(x\cos\theta - y\sin\theta)} + P_r e^{jk(x\cos\theta + y\sin\theta)}$$

1
...

$$\vec{H} = Y \left\{ P_i e^{-jk(x\cos\theta - y\sin\theta)} + P_r e^{jk(x\cos\theta + y\sin\theta)} \right\}$$

2

...

Where P_i and P_r are the amplitudes of the incident and reflected propagated waves respectively.

The boundary conditions on the tangential \vec{E} fields which have to be satisfied at matching-absorbing layer interface (G_1) are as follows:

$$G_1 \vec{E}^+ = G_1 \vec{E}^- = \vec{J}$$

$$\vec{H}^+ = \vec{H}^- = \vec{J}$$

$$\text{Also } K_p \sin \theta_p = K_q \sin \theta_q$$

Here + and - signs show the electric fields at opposite sides on matched lossy layer interface and \vec{J} is the current density in sheet. Further in Fig. 1, let p and q are the matching layer and lossy layer respectively.

Further electric field for p and q layer can be expressed as:

$$\vec{E}_p = P_{ip} e^{-jkp(x_p \cos \theta_{ip} + y \sin \theta_{ip})} + P_{rp} e^{-jkp(x_p \cos \theta_{rp} + y \sin \theta_{rp})}$$

3

...

$$\vec{E}_q = P_{iq} e^{-jq(x_q \cos \theta_{iq} + y \sin \theta_{iq})} + P_{rq} e^{-jq(x_q \cos \theta_{rq} + y \sin \theta_{rq})}$$

4

...

Starting from perfect electric conductor (PEC) layer at plane $x = 0$ where $P_i = 1$ and $P_r = -1$ passing through lossy absorbing layer and air-impedance matched layer with linear boundary transformation [15]

$$P_i = \frac{Z_o e^{jk_0 x_p \cos \theta_o}}{2 \cos \theta_o} \left[P_{ip} \left(\frac{\cos \theta_o}{Z_o} + \frac{\cos \theta_{ip}}{Z_p} + G_2 \right) e^{-jkp x_p \cos \theta_{ip}} + P_{rp} \left(\frac{\cos \theta_o}{Z_o} - \frac{\cos \theta_{rp}}{Z_p} + G_2 \right) e^{jkp x_p \cos \theta_{rp}} \right]$$

... (5)

$$P_r = \frac{Z_o e^{-jk_0 x_p \cos \theta_o}}{2 \cos \theta_o} \left[P_{ip} \left(\frac{\cos \theta_o}{Z_o} - \frac{\cos \theta_{ip}}{Z_p} - G_2 \right) e^{-jkp x_p \cos \theta_{ip}} + P_{rp} \left(\frac{\cos \theta_o}{Z_o} + \frac{\cos \theta_{rp}}{Z_p} - G_2 \right) e^{jkp x_p \cos \theta_{rp}} \right]$$

... (6)

Where x_p is the distance from the PEC layer to air-absorber interface and x_q is the distance from PEC layer to matched-lossy interface.

$k_0 = \omega_0 \sqrt{\epsilon_0 \mu_0}$; $k_p = k_0 \sqrt{\epsilon_{rp} \mu_{rp}}$ and $k_q = k_0 \sqrt{\epsilon_{rq} \mu_{rq}}$ are the wave numbers of free space, layer p and layer q respectively.

$$Z_0 = \frac{1}{Y_0} = 377\Omega$$

;

$$Z_p = \frac{1}{Y_p} = Z_0 \sqrt{\frac{\mu_p}{\epsilon_p}}$$

7

;

$$Z_q = \frac{1}{Y_q} = Z_0 \sqrt{\frac{\mu_q}{\epsilon_q}}$$

8

...

where Z_0, Z_p, Z_q are the impedance of free space, p layer and q layer respectively.

Reflection Coefficient of air-absorber interface is:

$$|\Gamma| = -20 \log_{10} \left| \frac{P_r}{P_i} \right|$$

9

...

In the current work, both layers (matching layer and lossy layer) are designed from epoxy resin loaded with reduced graphene particles but with different weight ratio. According to transmission line theory, the impedance of first layer i.e. matching layer must be approximately equal to free space impedance (377 ohm) [15]. This condition ensures the minimum reflection and maximum transmission of incident wave at air-absorber interface. To satisfy above, relative permittivity of the material should be equal to its relative permeability as seen from Eq. 7. Therefore a matching layer has been designed above absorbing layer, in which graphene oxide particles are blended in epoxy material with 5% weight ratio. This layer has 9.5 relative permittivity and 0.15 dielectric loss tangent particularly at 10 GHz frequency. Further the lossy/absorbing layer (next to matching layer) must possess high losses so as to absorb electromagnetic waves in terms of heat. For designing lossy layer, nanocomposites of graphene oxide particles blended in epoxy resin material with 15% weight ratio and 8 micrometer particle size has been proposed. This combination increases the relative permittivity of materials upto 18.5 and the dielectric loss tangent increased to 0.18 induces high losses to encountered electromagnetic waves [16]. Thus, most of the waves reaching to lossy layer dissipate and rest of the electromagnetic waves which manage to pass through lossy layer get fully reflected by perfect electric conductor layer which is placed at the back-end of absorber structure to ensure zero transmission.

The thickness of both the layers has been calculated on basis of quarter wavelength principle and it should be the odd multiple of quarter wavelength incident wave [17–18]. Therefore, for operating proposed electromagnetic absorber structure in X band, thickness of matching layer should be 2 mm and lossy layer is 0.5 mm backed by a perfect electric conductor sheet of negligible thickness.

To verify whether proposed absorber is insensitive to polarization, it has been illuminated with transverse electric (TE) and transverse magnetic (TM) polarization modes at different incident angles as depicted in Fig. 2 and Fig. 3.

3. Two-dimensional Antenna Array Geometry

Parallel to electromagnetic absorber, a 2×8 elements antenna array has also been designed using triangular conducting patches and aluminium oxide substrate with 9.8 relative dielectric constant as shown in Fig. 4.

For side lobe suppression of antenna array, the double layer rGO absorber will be integrated on same substrate. Due to absorber action means dissipating side lobe energy into heat, ambient temperature of array rises, which degrade the array performance. However, [30] suggests that aluminium oxide is one of the substrates on which the raised temperature effects are minimum as compared to commonly used substrates like Rogers or FR4. Therefore, in the proposed antenna array aluminium oxide substrate having 9.8 effective dielectric constant has been used. To resonate in X-band, dimensions are calculated analytically and enlisted in Table 1.

Table 1
Antenna array dimensions

| Parameter | Value |
|---|---------------------------------|
| Frequency band of operation | 8.2-12.4GHz |
| Resonating frequency | 10.2 GHz |
| Length and width (L×W) of Substrate | 13cm×12.8cm |
| Thickness of substrate | 0.254cm |
| Side length of equilateral triangular patch | 0.551cm |
| Width of corporate feed network | 6.35cm |
| Lumped port width | 0.35cm |
| Spacing within array elements | half wavelength ($\lambda/2$) |

4. Results And Discussion

Antenna arrays are attributed with high signal directivity, narrow beamwidth, less interference, high front to back ratio. All stated properties facilitate the signal to travel at larger distances and inherently achieved by increasing the number of array elements. But by increasing array elements, the number of side lobes as well as their levels increases due to transmission of electromagnetic wave from one element to another. Suppressing these intercoupling waves can drastically reduce the side lobe levels causing subsequent reduction in interference with major lobe. Placing the absorber structure in between array elements on same substrate can prove to be an industrially compatible approach which not only reduces the number of side lobes but the levels are also suppressed effectively. As the absorber structure is integrated with array elements on the substrate, extra hardware is therefore not required to implement this technique. The necessary condition to obtain the desired performance from absorber structure is that it should be frequency compatible with antenna array whose side lobes have to be suppressed and absorber structure must be polarization insensitive ensuring almost equal suppression of all electromagnetic waves incident at different angles. The reflection coefficient graphs of proposed double layer graphene oxides based absorber structure for TE polarized wave at normal and oblique angles has been shown in Fig. 5.

(both TE and TM modes)

As observed from figure, the proposed absorber structure has the desired reflection coefficient i.e. below -10 dB for whole X-band, particularly for TE mode. In addition absorber also covers Ku-band hence considered as wideband absorber. However, at 55° angle and above, the required reflection coefficient is not achieved at lower frequencies in X band. Further it can be observed that the reflection coefficient dip at normal incident angle ($\theta_i = 0^\circ$) reaches to -61.13 dB @11 GHz which tends to degrade as the incident angle increases. For 35°, this dip shifts to -55 dB @16 GHz and for 55° angle -40 dB @16 GHz reflection coefficient dip has been obtained.

In case of TM incidence of angles, it is evident that the reflection coefficient performance is not that better as in TE modes, but still for normal incidence angle (0°) and oblique angle (35°), value of reflection coefficient is below -10 dB for 8 GHz to 18 GHz range. For 55° TM incidence angle, the reflection coefficient is just below -10 dB in the range of the frequencies from 14 GHz to 16 GHz only. Thus absorber structure is not behaving as a good absorber at 55° and above that value of TM incidence angle.

Table 2 enlists the comparison between the proposed absorber structure and other absorbers reported in open literature. From table it can be observed that, proposed double layer absorber structure outperforms the existing single layer, double layer and multilayer absorber in terms of reflection coefficient and effective absorption bandwidth. Further to check the utility and effectiveness of the proposed absorber, it has been integrated with two-dimensional antenna array for suppression of array sidelobes which is a novel technique of interference mitigation [23, 24].

Table 2
Performance comparison of proposed absorber structure with reported absorbers

| Absorber composite material | Sample thickness | Operating frequency band | Reflection coefficient | Absorption bandwidth | Absorber validation | Ref. No. |
|---|---|--------------------------|--|--|------------------------------------|---------------|
| Multilayered Graphene deposited on quartz with PMMA spacers | six layered graphene/PMMA = 4.2 μ m | 26.5–40GHz. | --- | 50% absorption at 30 GHz | Not validated | 19 |
| Multilayered graphene sheets plus plasma medium | 1.65 cm | 10–100 GHz | -40 dB at 55 GHz | 97% absorption at 5 to 52 GHz | Not validated | 20 |
| Dual layer of CoFe ₂ O ₄ / PANI and calcined CoFe ₂ O ₄ | Two samples: 2mm and 2.5mm | 2–18 GHz | -19.0 dB at 16.2 GHz and -31.1dB at 12.8 GHz | Absorption bandwidth – 4.2 GHz (13.8 GHz to 18.0 GHz). | Not validated | 21 |
| Wax composite reduced graphene oxide hetrostructure nanosheets | 2.7mm | 2–18 GHz | -41.5 dB @ 9.5 GHz | 13.63 GHz (4.38 to 18 GHz) | Not validated | 22 |
| Dual layer epoxy resin loaded graphene oxide absorber | 2.5 mm | 2–18 GHz | -61.13 dB @11 GHz At TE normal incidence | 15.7 GHz (2.3 GHz to 18 GHz) | Validated on two-dimensional array | Proposed work |

For evaluating the performance of absorber structure on two dimensional triangular patch antenna array, absorber structures have been placed between interelement space of antenna array as shown in Fig. 5.

Absorber structure placed here will reduce the number of side lobes and their levels. The mechanism can be explained in terms of mutual coupling effect. Integrating absorber on array substrate will consequently reduce the mutual coupling introduced due to the transmission of electromagnetic waves from one element to another. After placing the interelement absorbers, antenna array radiates in far field region only; where the user may be present and the radiation in the close vicinity which interferes the amplitude and phase excitation of neighbouring elements (causes high side lobe levels) markedly reduces thus lowering sidelobe levels of antenna array.

Figure 7 shows the gain comparison plots of two-dimensional antenna array with and without interelement absorbers.

From figure, it can be observed that 14.14 dB gain has been achieved with two-dimensional 16 elements antenna array which is reasonably good. However the number of side lobes and their levels are get increased. Side lobe levels above - 10 dB would interfere the major lobe of antenna array and degrade its performance by decreasing front to back ratio and increasing bit error rate of array. After placing interelement absorber structure on same array substrate, the levels of first side lobes is significantly reduced from 5.248 dB to 2.518 dB and the ripples also diminish above 50° angle without changing the direction of major lobe. Further it can be observed that pattern symmetry of antenna array is also retained after integration of absorber which is also desirable parameter of antenna array.

Directivity comparison plots shown in Fig. 8 also validates the effectiveness of absorber structure for pattern enhancement and side lobe suppression of antenna array.

From directivity plot, it can be observed that the directivity of 14.23 dB @ 0° has been obtained with 16 elements of antenna array which remains unchanged after integration of interelement absorber. However, the side lobe levels are effectively reduced from 5.91 dB to 3.21 dB without changing major lobe direction and pattern symmetry of antenna array. Reduction in adjacent signal interference due to suppression of side lobes facilitate the target signal transmission and reception of antenna array.

5. Conclusion

In this paper, the double layer polarization insensitive graphene oxide based electromagnetic absorber has been proposed to reduce the number of side lobe and their levels for two-dimensional antenna array. The first layer or matching layer of absorber structure with dielectric loss tangent of 0.15 is designed so as to encounter less reflection at air-absorber interface. Further the lossy layer with 18.5 complex permittivity and 0.18 dielectric loss tangent ensures the dissipation of electromagnetic waves into heat when entered into absorber structure. To check the polarization insensitivity of absorber structure, various reflection coefficient plots have been drawn at TE and TM incidence normal and oblique angles. Reflection coefficient graphs authenticate that, at incident angles below 55° both in TE and TM waves, the reflection coefficient is below - 10 dB thus absorbing 90% of electromagnetic waves entering at different angles and polarization in absorber structure. Further - 61 dB @11 GHz reflection coefficient dip has been obtained at normal incident in TE mode with 2.5 mm sample thickness. For validation purpose, the proposed absorber structures have been integrated with two-dimension triangular patch antenna array resonates at 10.2 GHz. Placing absorber structures between interelement space of array elements suppresses the side lobe levels of antenna array from 5.24 dB to 2.51 dB thus enabling the array to transmit its signal at larger distance with interfering with adjacent signals. Therefore, proposed rGO based double layer polarization insensitive absorber can be utilized as an economical solution for advanced multi-function radar antenna array systems operating in X band.

Declarations

Author Contribution

All authors contributed to the study conception and design. Material preparation, data collection and analysis were performed by Surekha Rani, Anupma Marwaha and Sanjay Marwaha. The first draft of the manuscript was written by Surekha Rani. All authors read and approved the final manuscript. All authors contribute equally.

Acknowledgment

The authors are thankful to the Department of Electronics and Communication Engineering of Sant Longowal Institute of Engineering and Technology, Longowal, Sangrur for providing access to High Frequency Structural Simulator (HFSS) Software.

Conflicts of Interest

The authors declare no conflict of interest.

Funding

This research did not receive any specific grant from funding agencies in the public, commercial, or not-for-profit sectors.

Data Availability Statement

Data used to support the findings in this study are included within the manuscript.

References

1. Q. Liu, Q. Cao, H. Bi, C. Liang, K. Yuan, W. She, Y. Yang, R. Che: CoNi@SiO₂@TiO₂ and CoNi@Air@TiO₂ microspheres with strong wideband microwave absorption, *Adv. Mater.* 28. 486–490 (2016).
2. H. Lv, Z. Yang, S.J.H. Ong, C. Wei, H. Liao, S. Xi, Y. Du, G. Ji, Z.J. Xu: A flexible microwave shield with tunable frequency-transmission and electromagnetic compatibility, *Adv. Funct. Mater.* 29. 1900163 (2019). <https://doi.org/10.1002/adfm.201900163>.
3. X. Yan, D. Xue: Fabrication and microwave absorption properties of Fe_{0.64}Ni_{0.36}-NiFe₂O₄ nanocomposite, *Nano-Micro Lett.* 4. 176–179 (2012).
4. M.S. Cao, W.L. Song, Z.L. Hou, B. Wen, J. Yuan, The effects of temperature and frequency on the dielectric properties, electromagnetic interference shielding and microwave-absorption of short carbon fiber/silica composites, *Carbon* 48. 788–796 (2010).
5. H. Lv, Z. Yang, P.L. Wang, G. Ji, J. Song, L. Zheng, H. Zeng, Z.J. Xu: A voltage-boosting strategy enabling a low-frequency, flexible electromagnetic wave absorption device, *Adv. Mater.* 30. 1706343 (2018).
6. G. Wang, Z. Gao, S. Tang, C. Chen, F. Duan.: Microwave absorption properties of carbon nanocoils coated with highly controlled magnetic materials by atomic layer deposition. *ACS Nano*. 6. 11009–11017 (2012).
7. C. Chen, J. Xi, E. Zhou, L. Peng, Z. Chen, C. Gao: Porous graphene microflowers for high-performance microwave absorption, *Nano-Micro Lett.* 10. 26-34 (2018).
8. C. Li, Q. Cao, F. Wang, Y. Xiao, Y. Li, J. Delaunay: H. Zhu, Engineering graphene and TMDs based van der Waals heterostructures for photovoltaic and photoelectrochemical solar energy conversion, *Chem. Soc. Rev.* 47. 4981–

- 5037 (2018).
9. P. Liu, Y. Huang, J. Yan, Y. Yang, Y. Zhao: Construction of CuS nanoflakes vertically aligned on magnetically decorated graphene and their enhanced microwave absorption properties, *ACS Appl. Mater. Interfaces* 8. 5536–5546 (2016).
 10. A. Gupta, T. Sakthivel: S. Seal, Recent development in 2-D materials beyond graphene, *Prog. Mater. Sci.* 73. 44–126 (2015).
 11. Renchao Hu, Guoguo Tan, Xisheng Gu, Shuwen Chen, Chenguang Wu, Qikui Man, Chuntao Chang, Xinmin Wang, Run-Wei Li, Shenglei Che, Liqiang Jiang: Electromagnetic and microwave-absorbing properties of Co-based amorphous wire and Ce₂Fe₁₇N₃-d composite, *Journal of Alloys and Compounds*, 730. 255-260 (2018).
 12. Ruixiang Deng, Ke Zhang, Meiling Li, Lixin Song, Tao Zhang: Targeted design, analysis and experimental characterization of flexible microwave absorber for window applications, *Materials and Design*. 162. 119–129 (2019).
 13. Guangzhen Cui, Yanli Lu, Wei Zhou, XuliangLv, Jiangnan Hu, Guoyu Zhang and Guangxin Gu: Excellent Microwave Absorption Properties Derived from the Synthesis of Hollow Fe₃O₄@ReducedGraphite Oxide (RGO) Nanocomposites, *Nanomaterials*. 9. 1-12 (2019).
 14. Hesham A. El-Hakim, K. R. Mahmoud, and A. A. Abdelaziz: Design of Compact Double-Layer Microwave Absorber for X-Ku Bands Using Genetic Algorithm, *Progress in Electromagnetics Research B*. 65. 157–168 (2016).
 15. Knott, E. F., J. F. Shaffer, and M. T. Tuley: *Radar Cross Section*, Artech House, London, (1993).
 16. Kevin Rubrice, Xavier Castel, Mohamed Himdi and Patrick Parneix: Dielectric Characteristics and Microwave Absorption of Graphene Composite Materials, *journal of materials*. 825. 1-10 (2016).
 17. Queffelec, P., G. Philippe, J. Gieraltowski, and J. Loaec: A microstrip device for the broadband simultaneous measurement of complex permeability and permittivity. *IEEE Transactions on Magnetics*. 30. 224–231 (1994).
 18. William, W. B.: Automatic measurement of complex dielectric constant and permeability at microwave frequencies, *IEEE Proceeding*. 62. 33–36 (1974).
 19. Gelza M. Barbosa, Marbey M. Mosso, Cecilia Vilani, Dunieskys R. G. Larrud Eric C. Romani, and Fernando L. F. Junior: Graphene Microwave Absorber, Transparent, Lightweight, Flexible, and Cost-Effective, *Microwave and Optical Technology Letters*. 56. 560-566 (2014).
 20. Mahdi Rahmanzadeh, Hamid Rajabalipanah, and Ali Abdolali: Analytical Investigation of Ultrabroadband Plasma–Graphene Radar Absorbing Structures, *IEEE Transactions on Plasma Science*. 45. 945-954 (2017).
 21. Yewen Xu, Guozhu Shen, Hongyan Wu, Bin Liu, Xumin Fang, Ding Zhang, Jun Zhu: Double-layer microwave absorber based on nanocrystalline CoFe₂O₄ and CoFe₂O₄/PANI multi-core/shell composites, *Materials Science-Poland*. 35. 94-102 (2017).
 22. Deqing Zhang, Tingting Liu, Junye Cheng, Qi Cao, Guangping Zheng, Shuang Liang, Hao Wang, Mao-Sheng Cao: Lightweight and High-Performance Microwave Absorber based on 2D WS₂–RGO Heterostructures, *Nano-micro letters*. (2019), <https://doi.org/10.1007/s40820-019-0270-4>
 23. Surekha Rani, Anupma Marwaha, Sanjay Marwaha: Utilization of graphene oxide-based microwave absorber for pattern enhancement of patch antenna array. *J. Nanophoton*. **12**. 036012(1-13) (2018). doi: 10.1117/1.JNP.12.036012.
 24. Surekha Rani, Anupma Marwaha, Sanjay Marwaha, Sukhleen Bindra, Murthy Chavali & P. Narasimha Reddy: Synthesis and Validation of a Cu Meta-Based Wideband Microwave Absorber on an Antenna Array. *Journal of Electronic Materials*. 42. 2019 (2019).

25. S. Bykkam, V.K. Rao, S.C. Chakra, T. Thunugunta: A Review: Synthesis Methods of Graphene and its Application in Supercapacitor Devices. *J. Inter., Adv. Biotechnol. Res.* 4, 142–146 (2013)
26. Llatser, I., Kremers, C., Chigrin, D.N., Jornet, J.M: Characterization of Graphene-based Nano-antennas in the Terahertz Band. 6th European Conference on Antennas and Propagation (EUCAP), Prague, Czech Republic (2012)
27. Wu, B.; Tuncer, H.M.; Naeem, M.; Yang, B.; Cole, M.T.; Milne, W.I.; Hao, Y.: Experimental demonstration of a transparent graphene millimetre wave absorber with 28% fractional bandwidth at 140 GHz. *Sci. Rep.*, 4, 4130 (2014)
28. Geim, A.K., Novoselov, K.S.: The rise of graphene. *Nat. Mater.* 6(3), 183-191 (2007) [http://dx.doi.org/10.1038/nmat1849]
29. Kelan Yan, a Feng Yin: Broadband microwave absorber constructed by reduced graphene oxide/La_{0.7}Sr_{0.3}MnO₃ composites. *RSC advances* 9, 41817–41823 (2014).
30. Surekha Rani, Anupma Marwaha, Sanjay Marwaha: Investigation of substrate materials for graphene oxide absorber loaded antenna array increased ambient temperature, *J. photonic network communication. J. photonic network communication*, Springer, 40, 94-102 (2020).

Figures

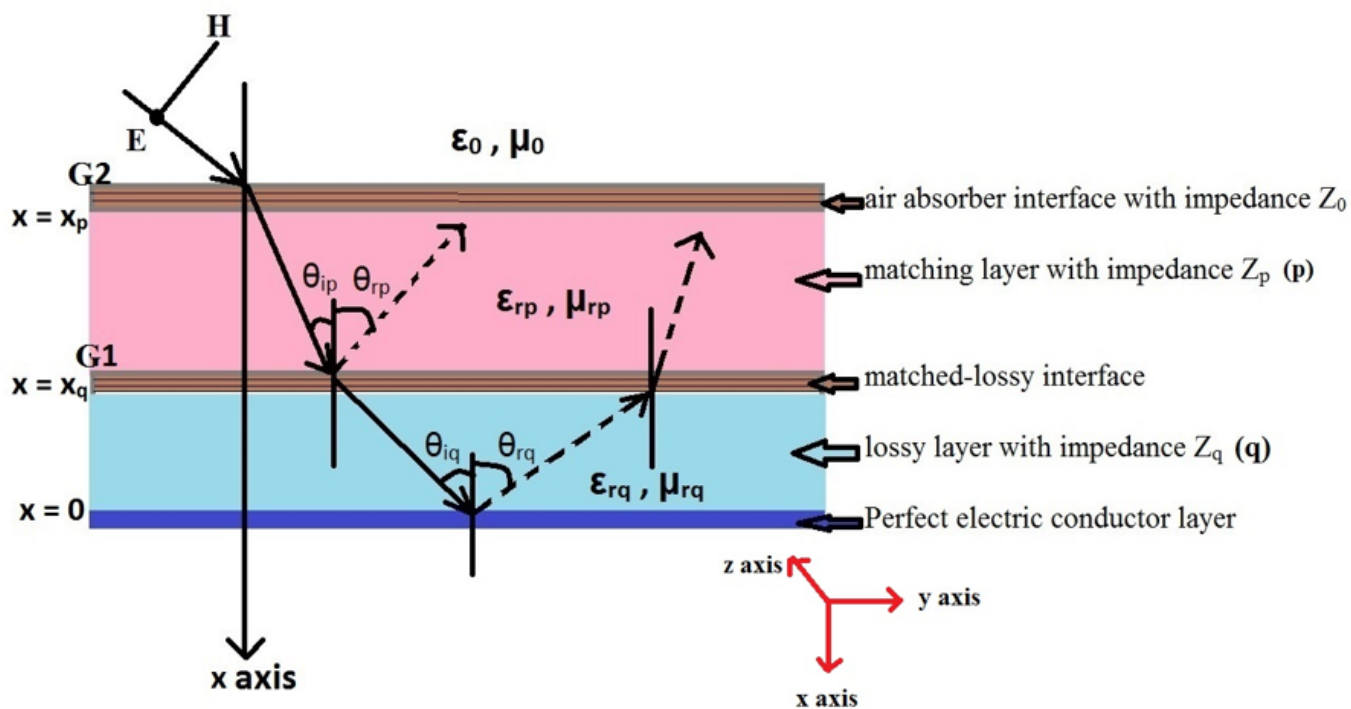


Figure 1

Wave model of dual layer reduced graphene oxide absorber [15]

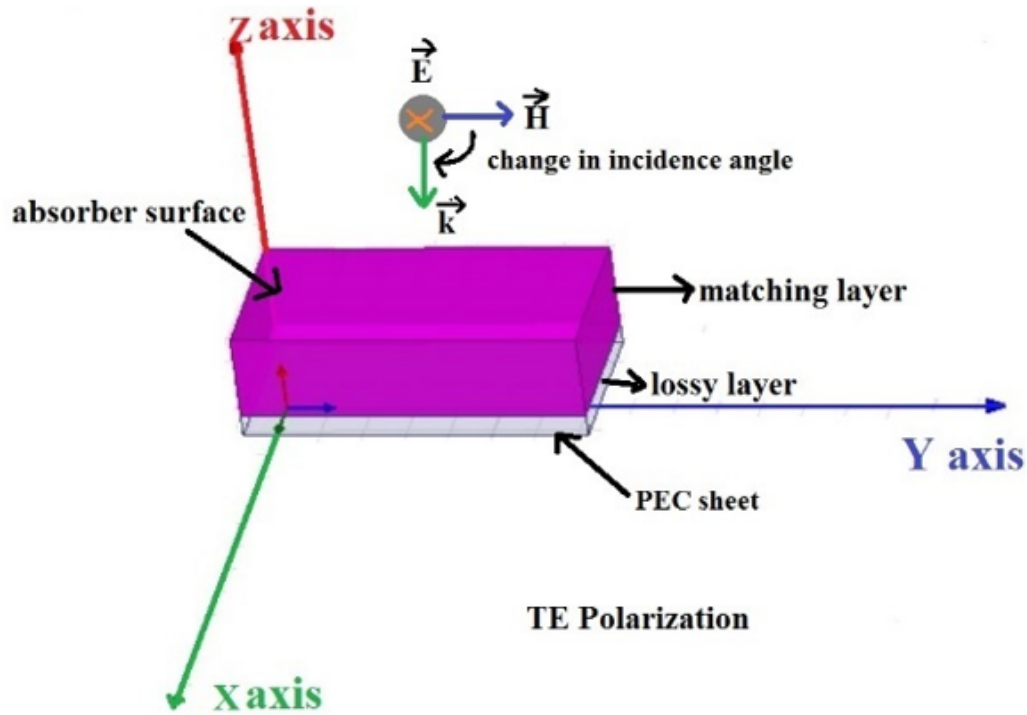


Figure 2

Absorber structure with TE polarized wave

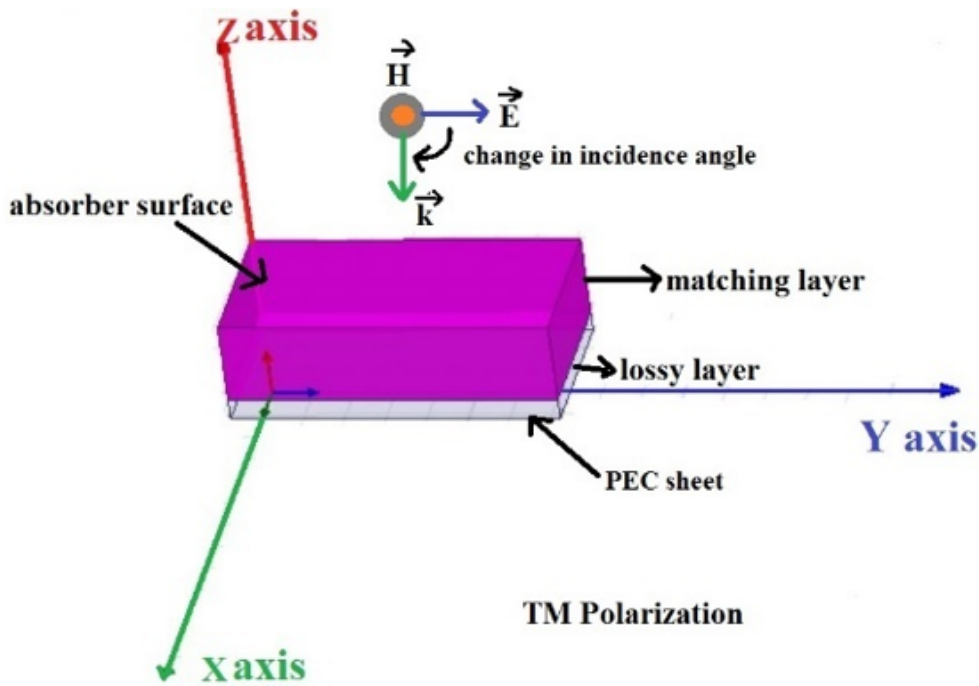


Figure 3

Absorber structure with TM polarized wave

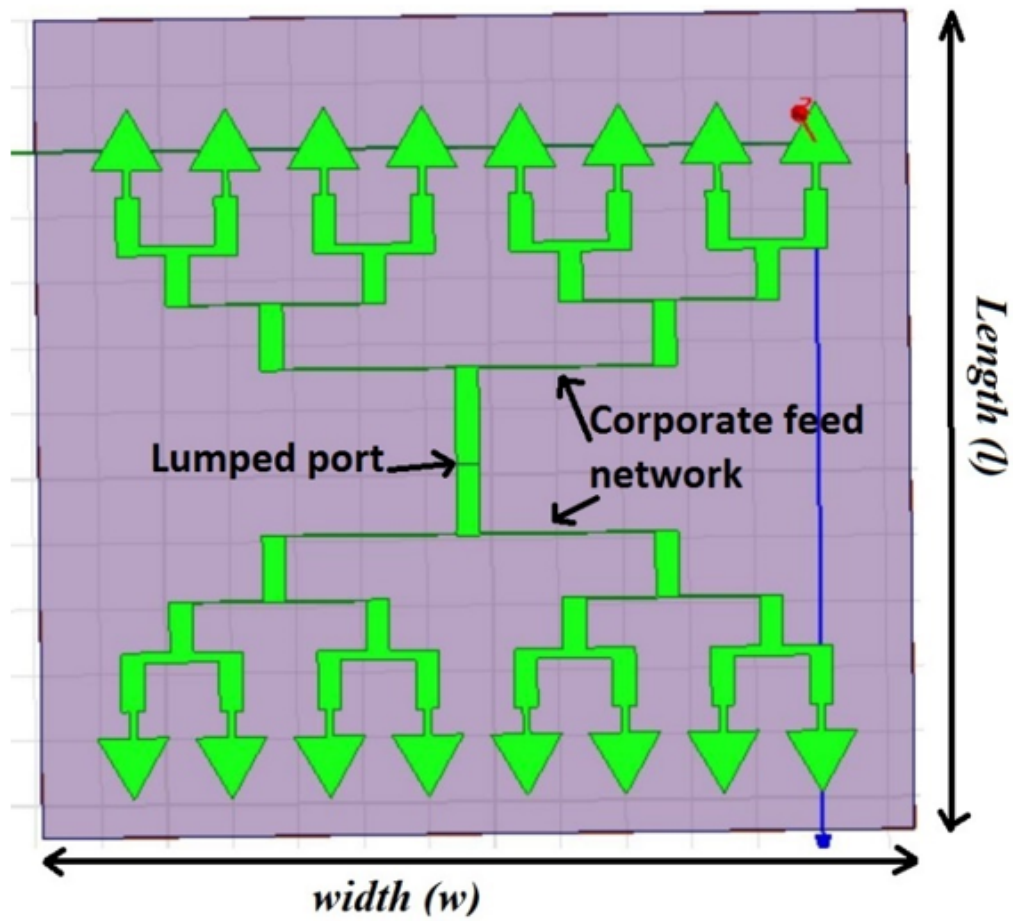


Figure 4

2x8 elements triangular patch array

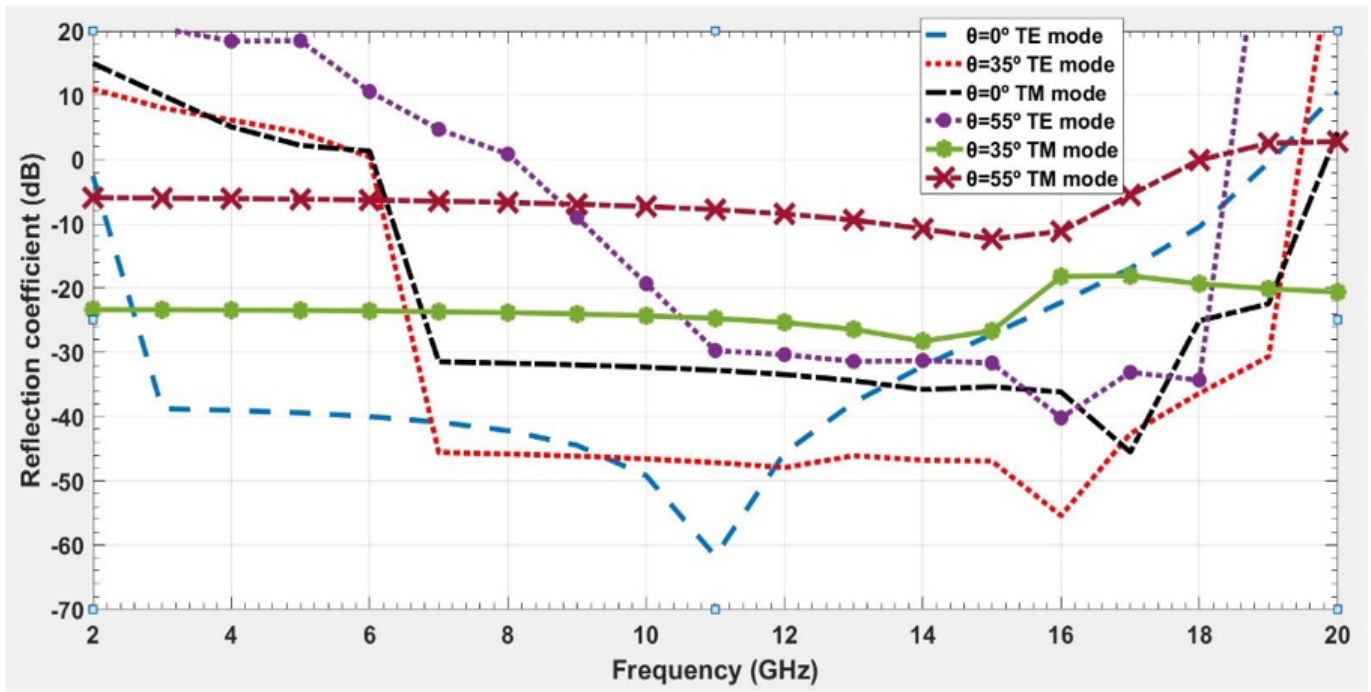


Figure 5

Reflection coefficient of double layer absorber at different incident angles

(both TE and TM modes)

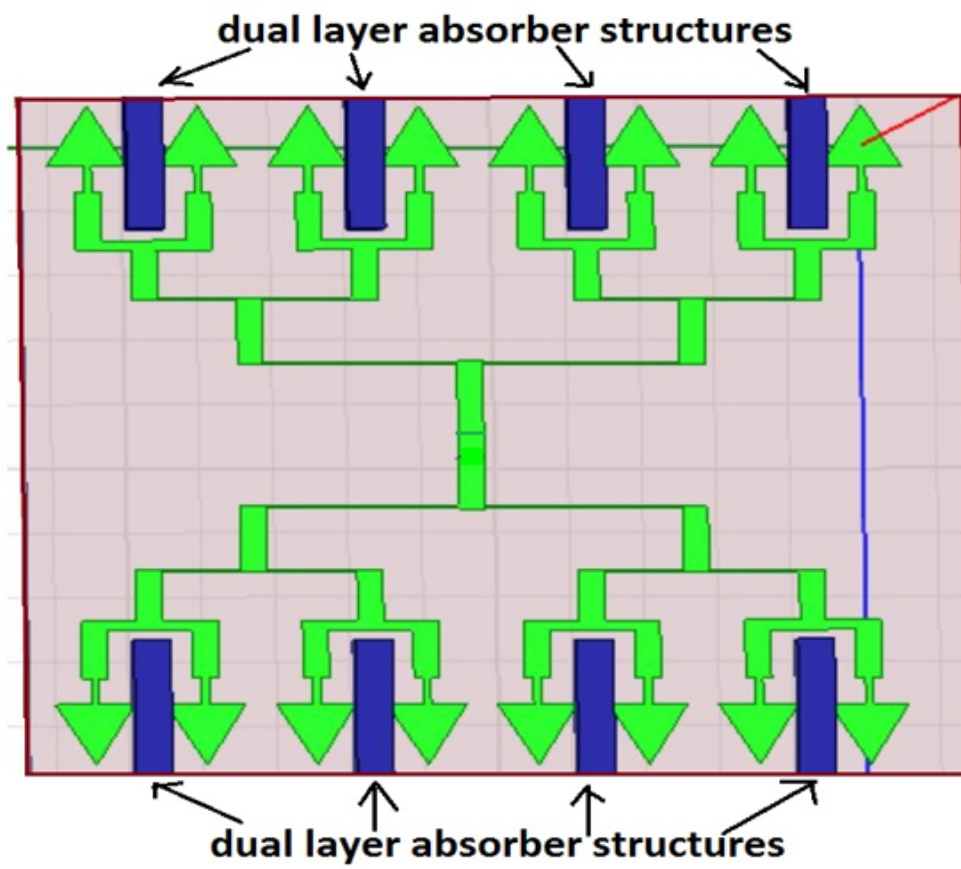


Figure 6

2x8 elements triangular patch array integrated with double layer absorber structure

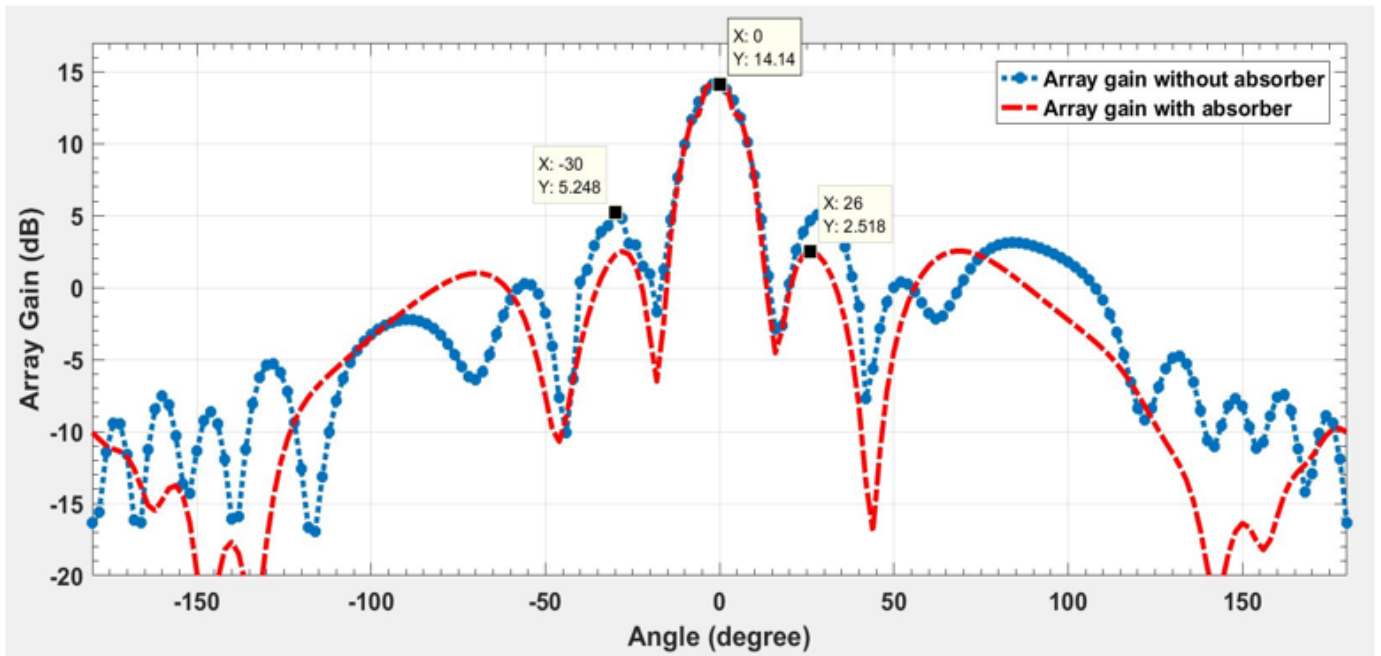


Figure 7

Gain comparison plot of antenna array with and without interelement absorbers

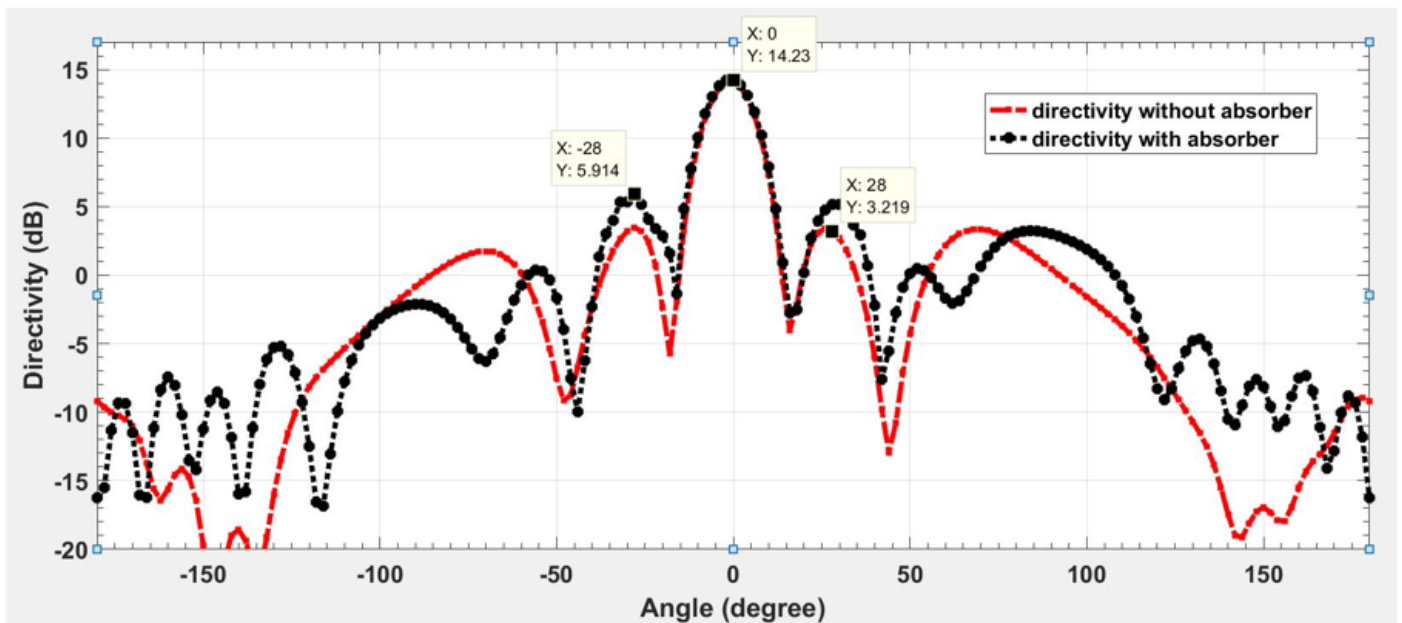


Figure 8

Directivity comparison plot of antenna array with and without interelement absorbers